5-503.32

1769

Response to review comments on "Development and Verification of VAM3DF,a Numerical Flow and Transport Modeling Code" by Dr. Sam Lee, Department of Energy.

General Comments:

Comment #: 1 Commentor: S. Lee Section #: Page #: Title

The title has been changed to "Development and Verification of VAM3DF; a Numerical Code for Modeling Flow and Transport in Groundwater". See title page.

Comment #: 2 Commentor: S. Lee Section #: Page #:

In Phases II and III, Data Fusion will be used to update model parameters based on site observations. Comparison with site observations will be an integral part of the process.

Comment #: 3 Commentor: S. Lee Section #: Page #:

Layer 1 had the highest concentration throughout the simulation. Hence, it was used in the comparison between SWIFT and VAM3DF. In response to Dr. Lee's comment, Figures 1 through 12 are included here to show uranium concentration in all model layers for Run B1.

Comment #: 4 Commentor: S. Lee Section #: Page #:

Variable names in equations and in the text are now in italics.

Specific Comments:

Comment #: 1 Commentor: S. Lee Section #: 1.1 Page #: 1-1

The statement has been changed to "Table 1.1 shows a comparison of the advantages of VAM3DF with MODFLOW-SURFACE, MT3D96, and MODFLOWT. See Page 1-2.

Comment #: 2 Commentor: S. Lee Section #: 1.1 Page #: 1-3

The developer of each code has been added to Table 1.1. See Page 1-3.

Comment #: 3 Commentor: S. Lee Section #: 2.1 Page #: 2-1

The statement "and finite difference" has been added. See Page 2-1.

1

Comment #: 4 Commentor: S. Lee Section #: 2.1 Page #: 2-1

The statement clearly indicates that the steady-state simulation is performed by solving the steady-state form of the governing equation while the transient simulation is carried out by time marching. In time marching, the transient form of the governing equation is solved at discrete points in time starting from the initial conditions. In this approach, the solution at a specific time level depends on the conditions in the previous time level and the solution proceeds until the target time is reached. Such an approach is different from methods that utilize Laplace transform, where the solution at the target time can be obtained directly from the initial condition without the need for intermediate time stepping.

Comment #: 5 Commentor: S. Lee Section #: 2.3.3 Page #: 2-14

Equation 2.27 has been corrected. See page 2-14.

Comment #: 6 Commentor: S. Lee Section #: 3.5 Page #: 3-15

The two paragraphs have been modified to further explain the application of the DFM in the estimation of dispersivity. The implementation of Data Fusion to transport simulation will be carried out in Phase II. The approach used will be discussed in more details in Phase II.

Comment #: 7 Commentor: S. Lee Section #: 3.5 Page #:

DFM is a parameter estimation technique into which physically based constraints (such as section 3.2) are incorporated. The DFM will be used to minimize the difference between observed and predicted concentrations in space and time. Details of the DFM will be discussed in Phase II documentations.

Comment #: 8 Commentor: S. Lee Section #: 3.5 Page #:

See response to comment 7 above.

Comment #: 9 Commentor: S. Lee Section #: 5.2 Page #: 5-1

Equation 5.1 in its current form is correct. The term Q has been defined in the text as the volumetric source/sink flux (L^3/T).

Comment #: 10 Commentor: S. Lee Section #: 7.2 Page #: 7.1

For block centered models, the total number of elements will be equal to the total number of nodes. Hence, a model with 10 elements in the x direction and 10 element in the y direction will require 10x10 nodes. To represent the same number of elements (100) using a mesh-centered model requires adding one row and one column of nodes. As a result, the total number of nodes will be 11 x 11 (see figure below). Because VAM3DF

uses a mesh-centered grid, the model requires 121x113 nodes to represent the same number of elements as those used in the SWIFT GMA model. However, to avoid relocating the nodes used in SWIFT GMA model, the same nodes (120x112) were used. Thereby, reducing the spatial extent of the domain to 14,875 ft by 13875 ft.

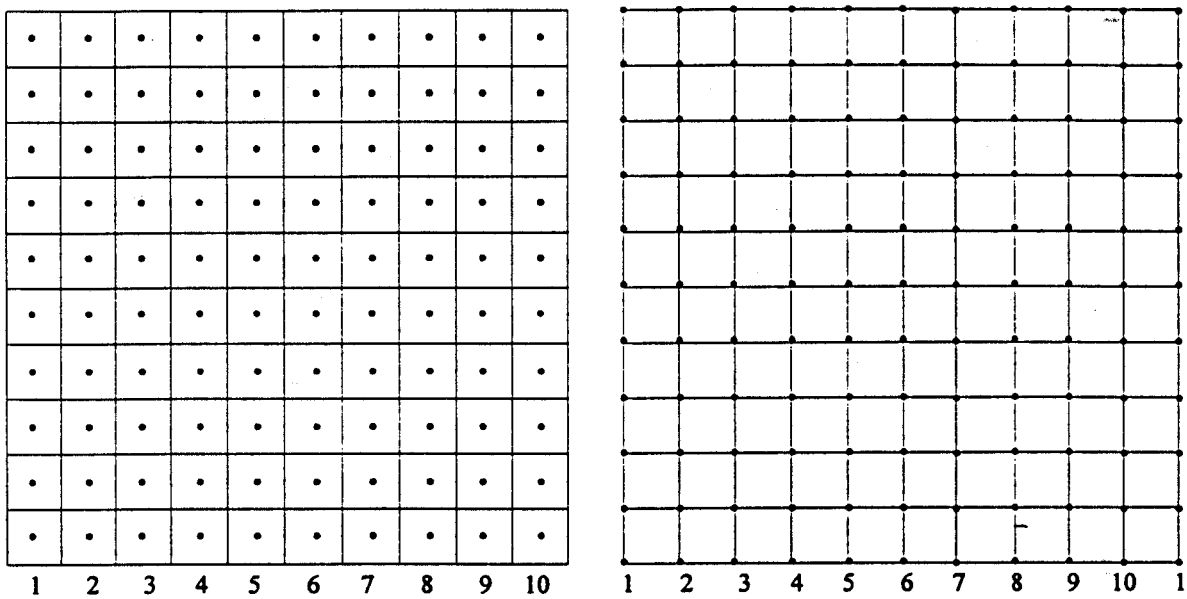

Comment #: 11 Commentor: S. Lee Section #: 7.2 Page #: 7.5

A new paragraph has added to explain the choice of the desorption rates.

Comment #: 12 Commentor: S. Lee Section #: 7.4.1 Page #: 7-35

The paragraph has been modified.

Comment #: 13 Commentor: S. Lee Section #: 7.4.2 Page #: 7-57

There were no experimental data to support the choice of values for chemisorption rate. However, desorption batch experiments have shown that a considerable portion of uranium mass remained on the solid phase after reaching equilibrium. The paragraph on page 7-57 was modified to explain the estimated values of chemisorption.

Comment #: 14 Commentor: S. Lee Section #: 7.4.2 Page #: 7-57

From the mass balance calculation of the earlier runs (D1 and D2), it was obvious that the initial sorbed mass was high. It is known from the literature that the sorption capacity of the aquifer material is usually limited. As a result, the relationship was chosen in such a way that the sorption capacity of the aquifer material decreases as the dissolved concentration increases. Additional explanation has been provided on page 7-57.

Comment #: 15 Commentor: S. Lee Section #: 7.4.2 Page #: 7-65

A simple calculation will show that a desorption rate of 0.01 (1/day) reflects a half-life of 70 days which is fast compared to 10 year.

Comment #: 16 Commentor: S. Lee Section #: 7.4.2 Page #: 7-67

The paragraph on page 7.67 has been modified to explain the mass distribution in Figure 7.47.

4

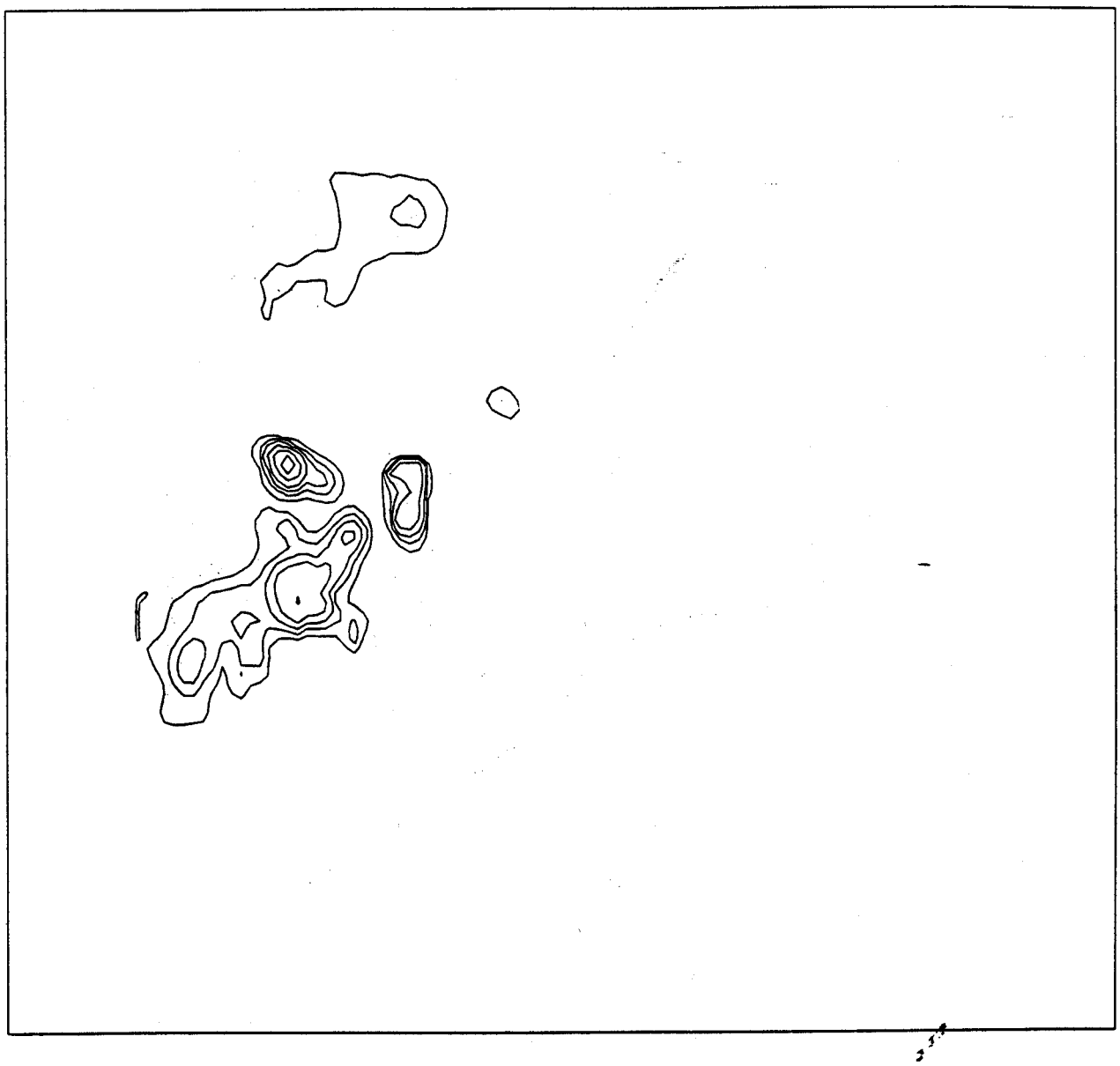

Figure 1 **Concentration in the upper node of layer 2 (1997). Contours are in 20, 50, 100, 200, 500, 1000, and 2000 ppb (Run B1).**

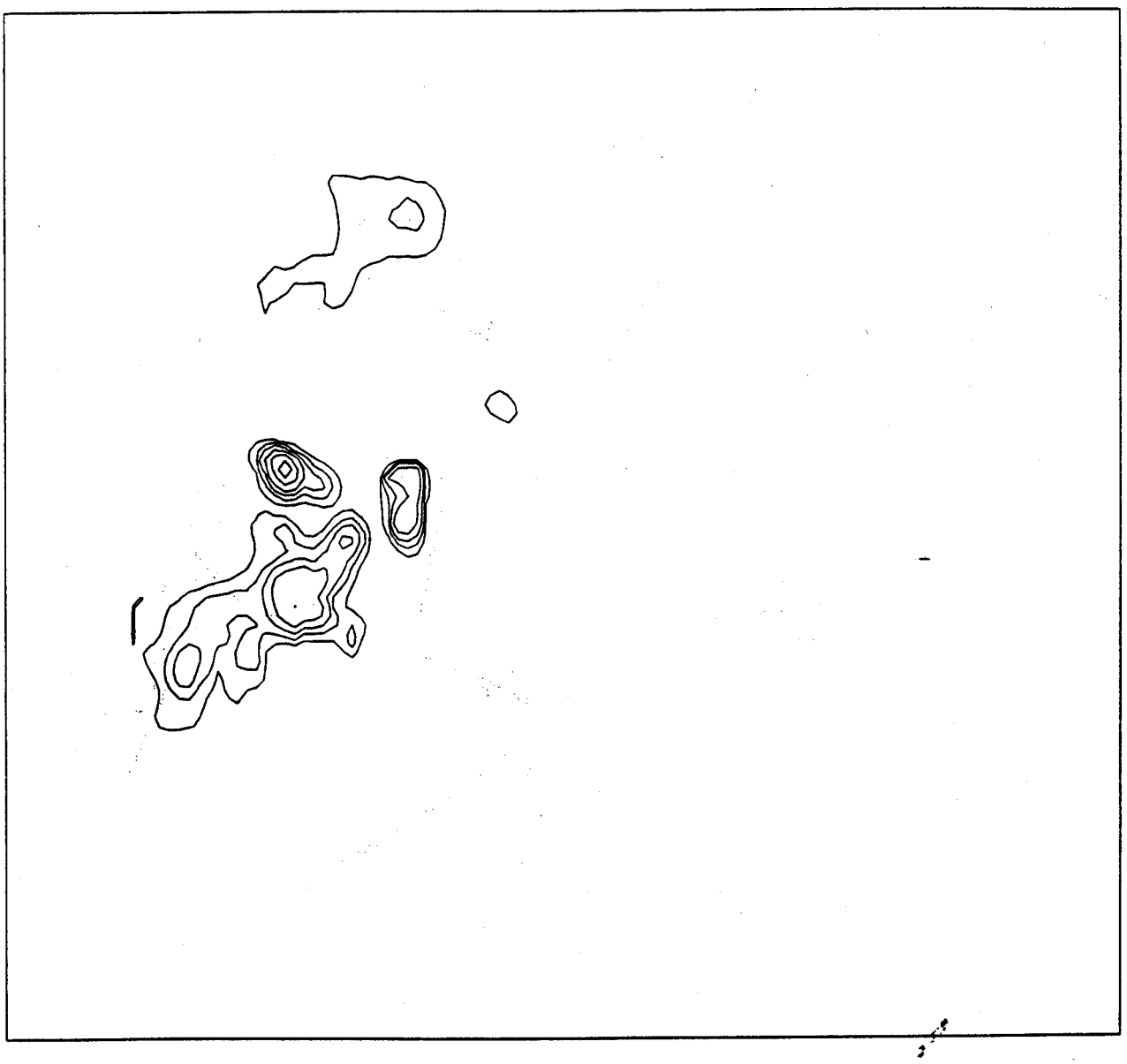

— 20 — Concentration in ppb.

• Well.

2000 0 2000 4000 ft

Figure 2 Concentration in the lower node of layer 2 (1997). Contours are in 20, 50, 100, 200, 500, 1000, and 2000 ppb (Run B1).

6

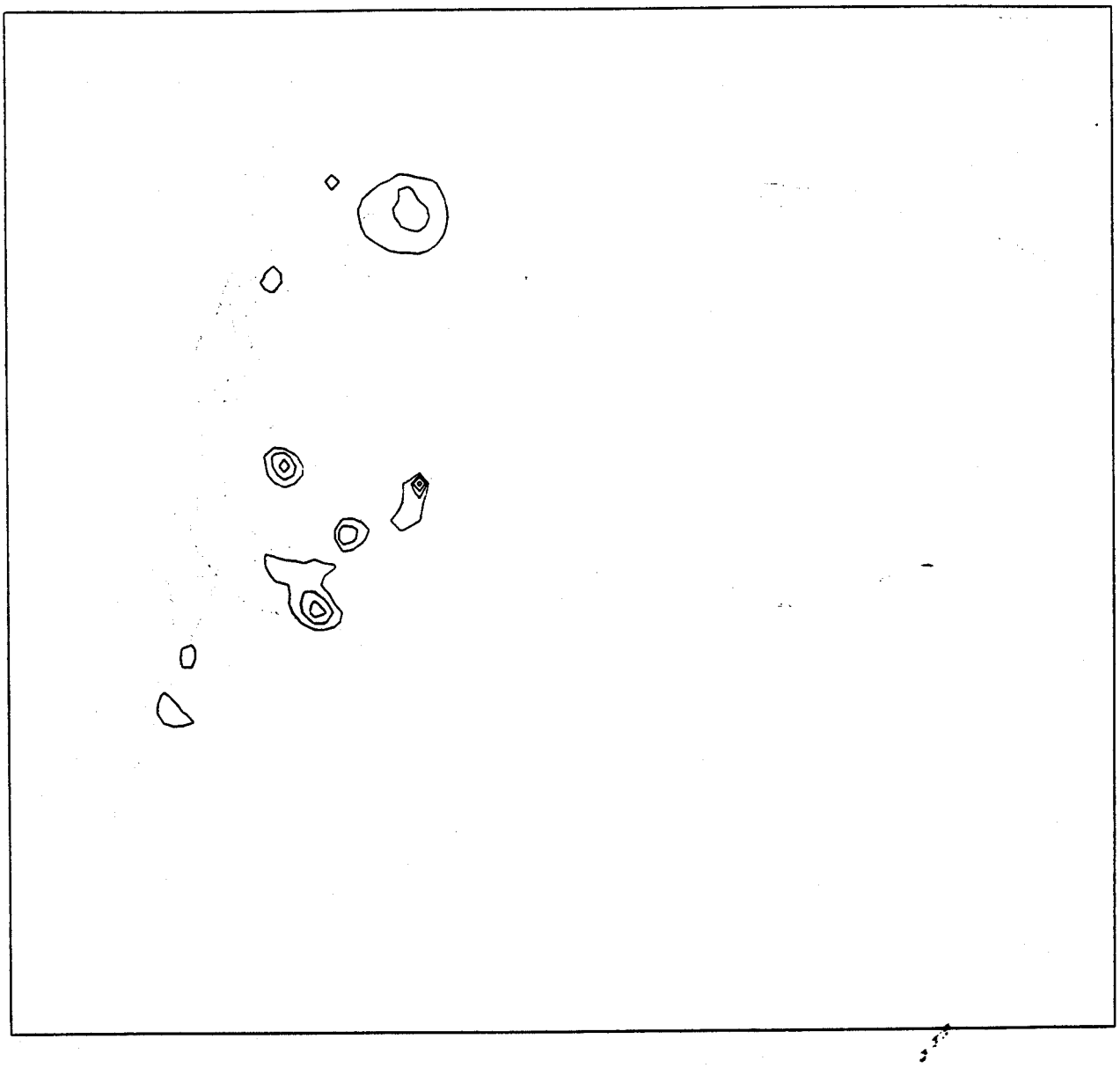

— 20 — Concentration in ppb.

• Well.

Figure 3 Concentration in the upper node of layer 3 (1997). Contours are in 20, 50, 100, 200, 500, 1000, and 2000 ppb (Run B1).

7

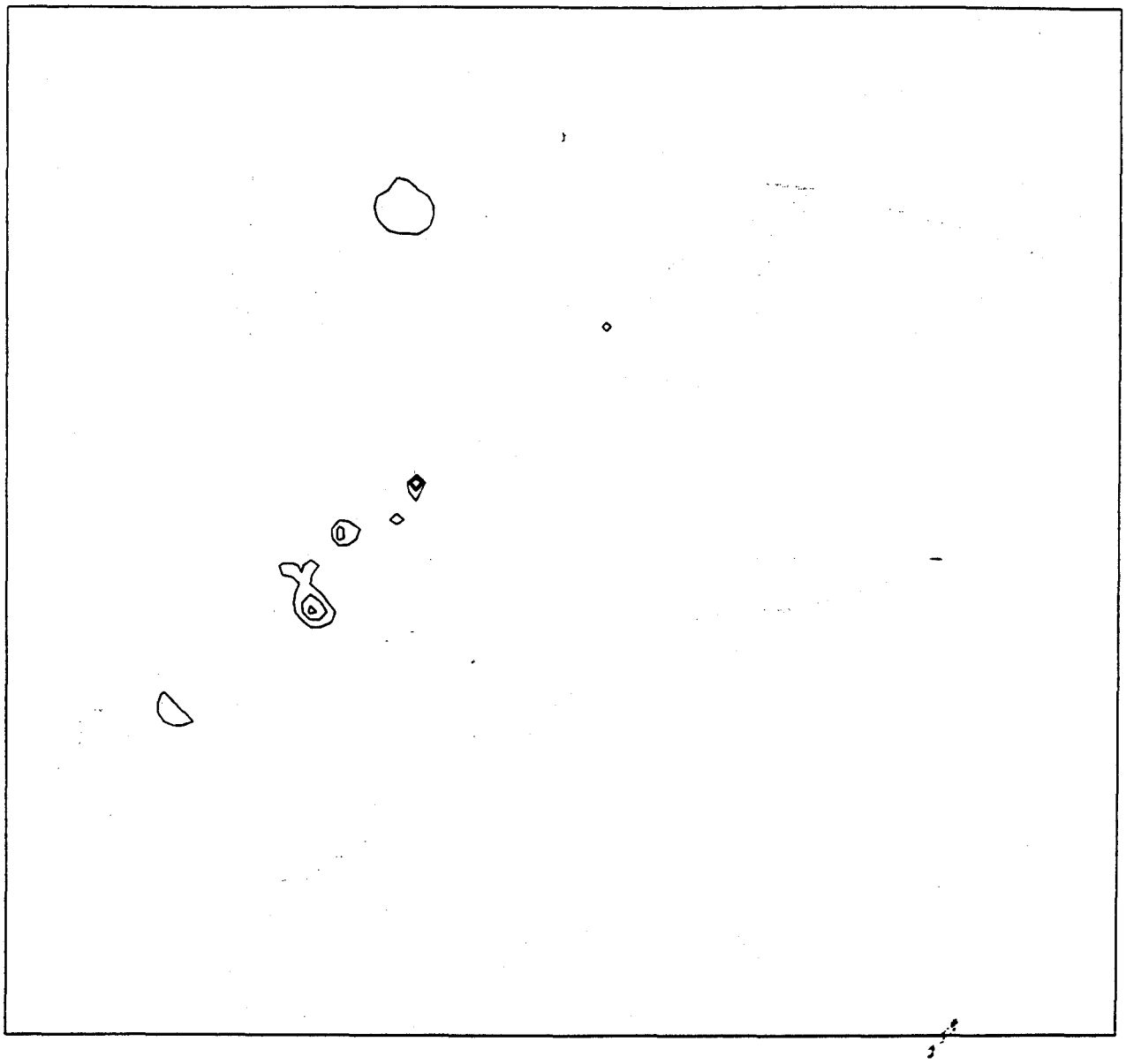

— 20 — Concentration in ppb.

• Well.

2000 0 2000 4000 ft

Figure 4 Concentration in the Lower node of layer 3 (1997). Contours are in 20, 50, 100, 200, 500, 1000, and 2000 ppb (Run B1).

8

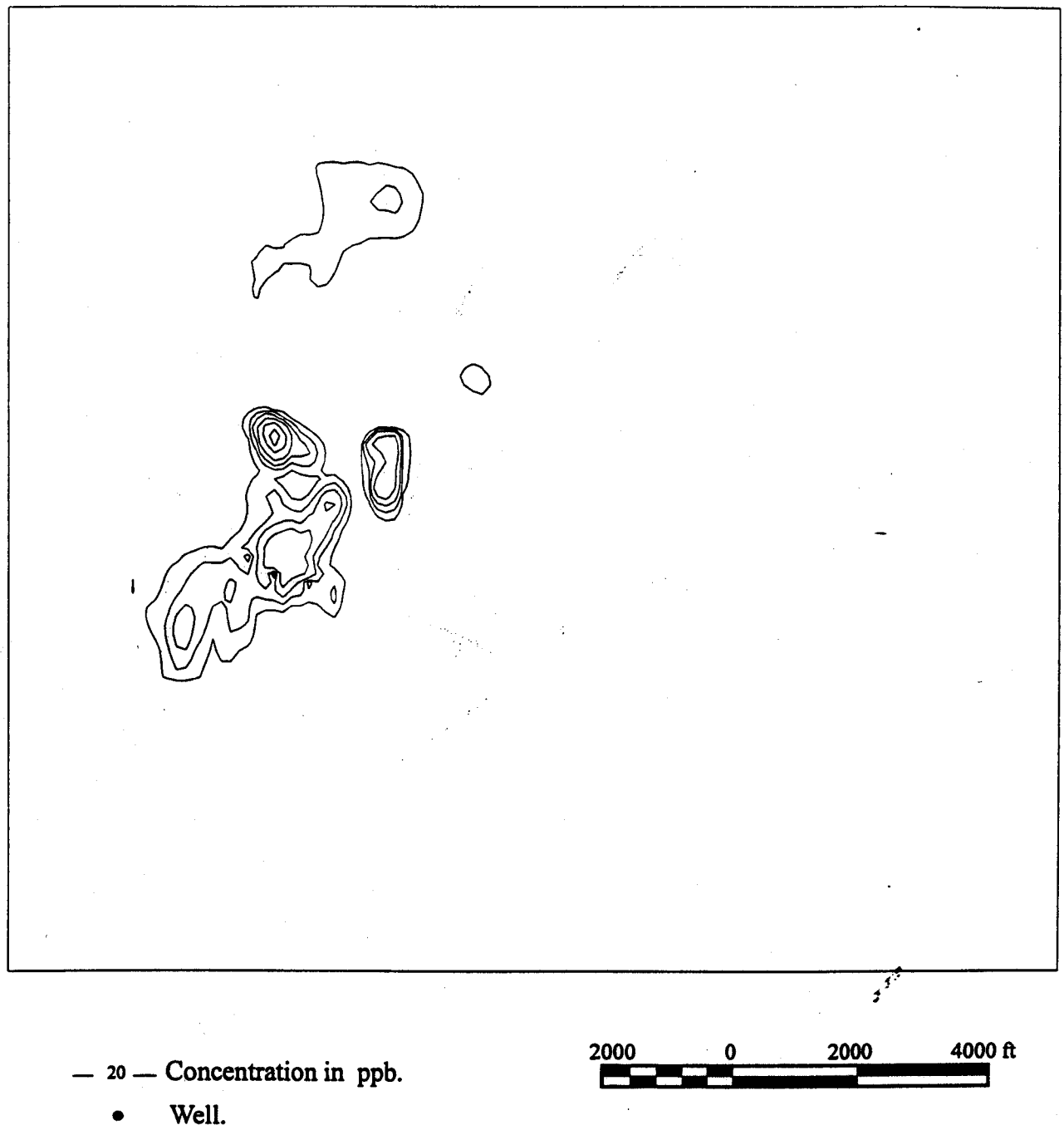

Figure 5 Concentration in the upper node of layer 2 (1998). Contours are in 20, 50, 100, 200, 500, 1000, and 2000 ppb (Run B1).

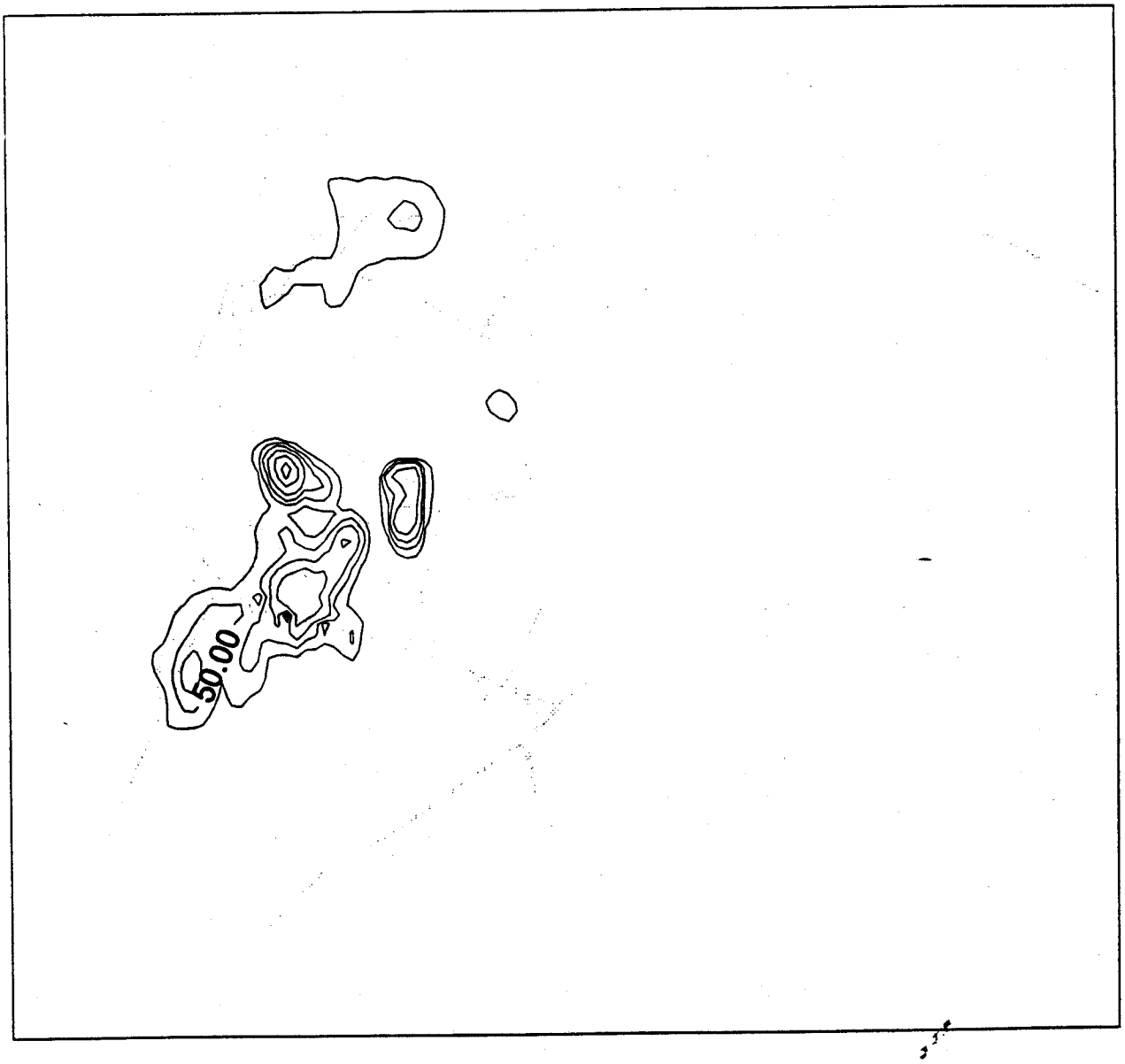

Figure 6 **Concentration in the lower node of layer 2 (1998). Contours are in 20, 50, 100, 200, 500, 1000, and 2000 ppb (Run B1).**

10

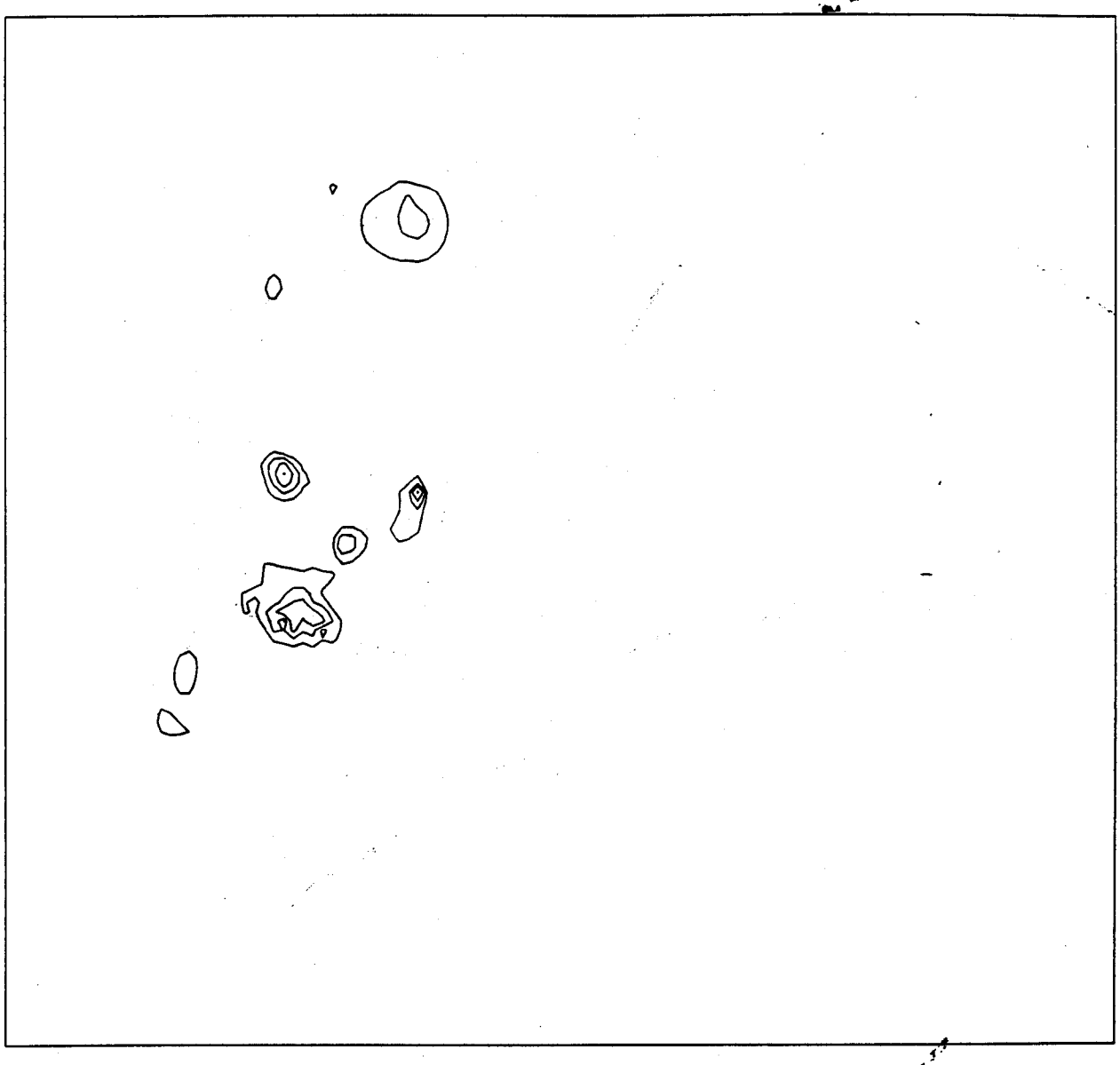

— 20 — Concentration in ppb.

• Well.

2000 0 2000 4000 ft

Figure 7 Concentration in the upper node of layer 3 (1998). Contours are in 20, 50, 100, 200, 500, 1000, and 2000 ppb (Run B1).

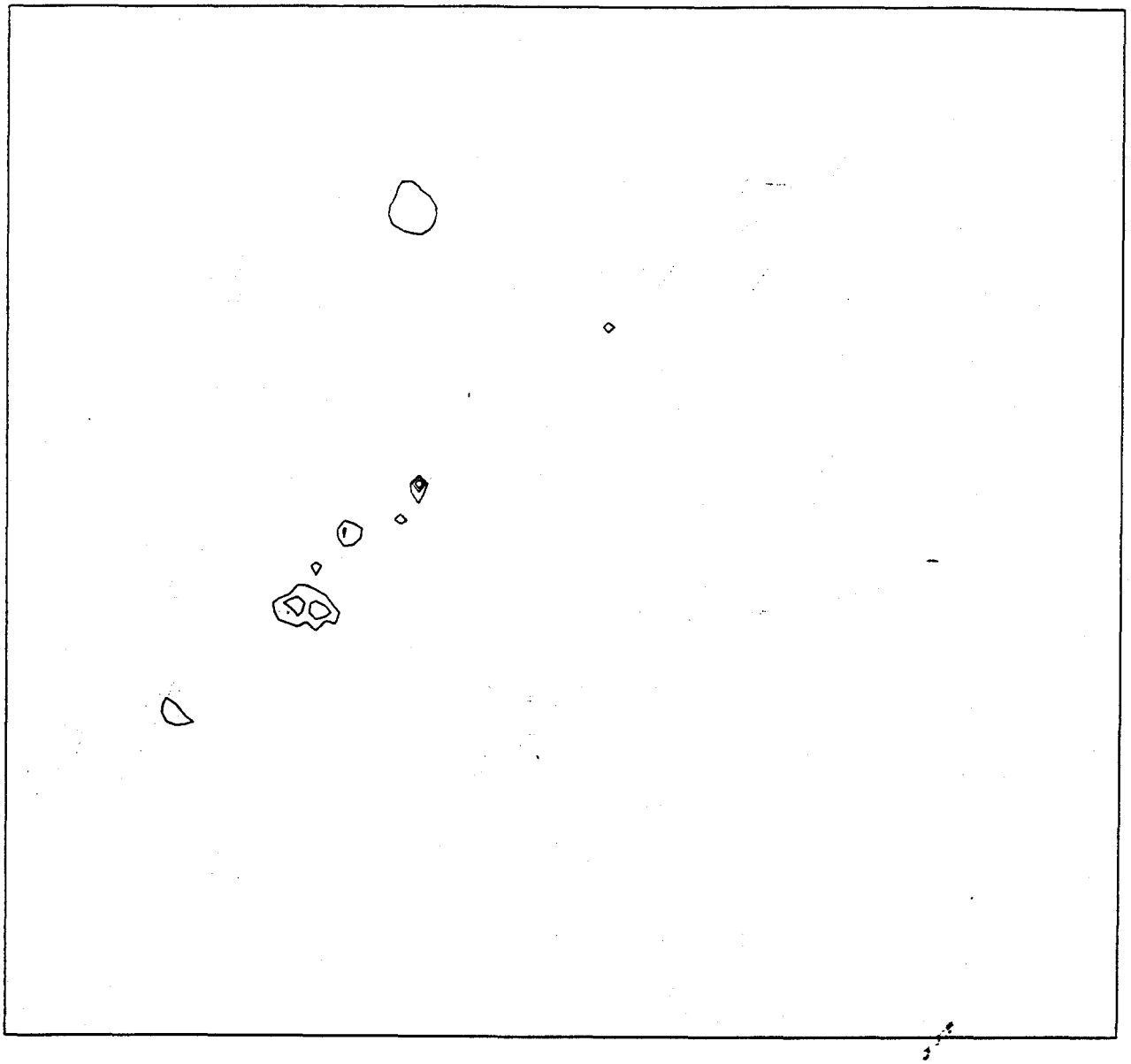

— 20 — Concentration in ppb.

• Well.

2000 0 2000 4000 ft

Figure 8 Concentration in the Lower node of layer 3 (1998). Contours are in 20, 50, 100, 200, 500, 1000, and 2000 ppb (Run B1).

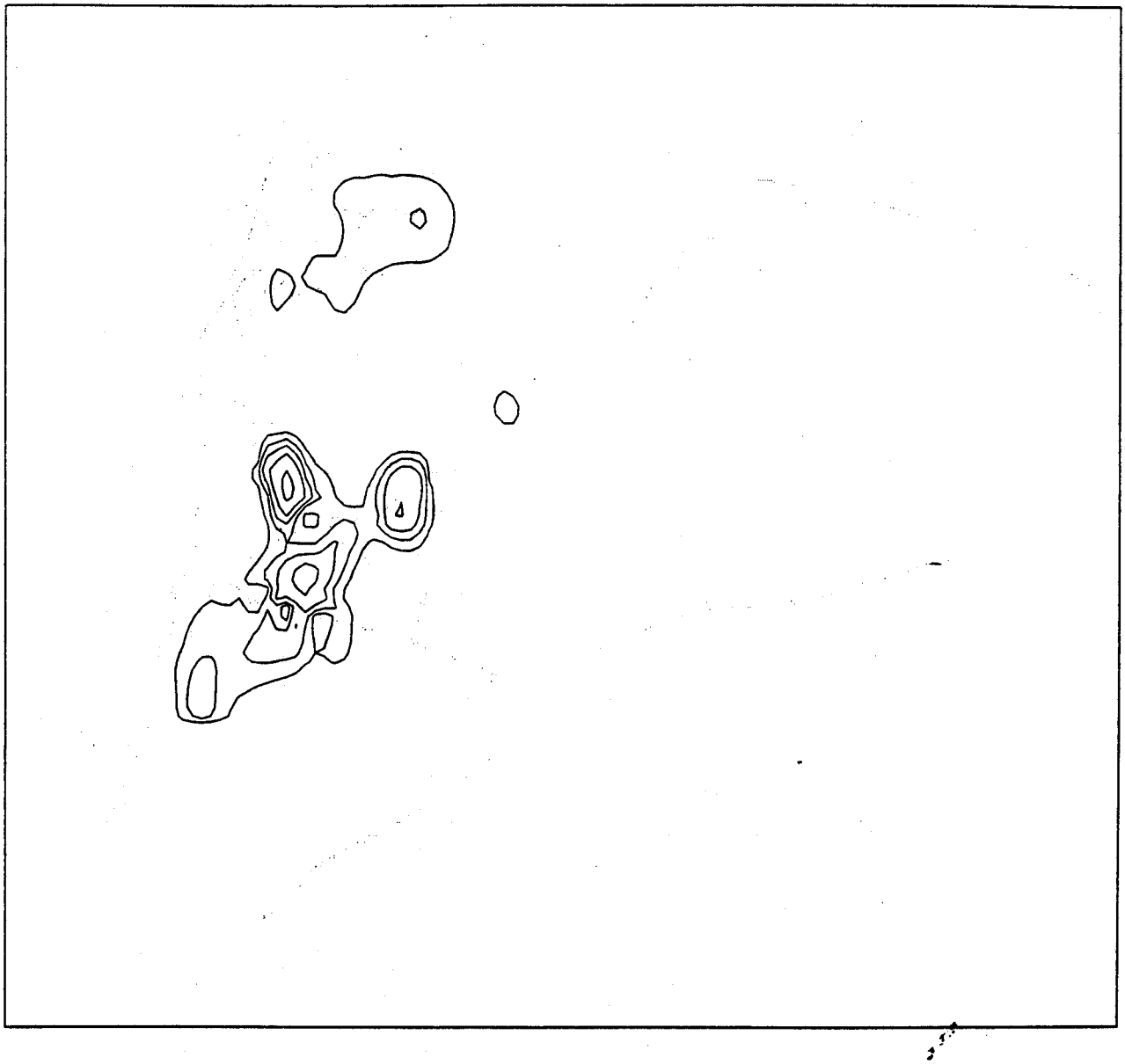

— 20 — Concentration in ppb.

• Well.

2000 0 2000 4000 ft

Figure 9 Concentration in the upper node of layer 2 (2003). Contours are in 20, 50, 100, 200, 500, 1000, and 2000 ppb (Run B1).

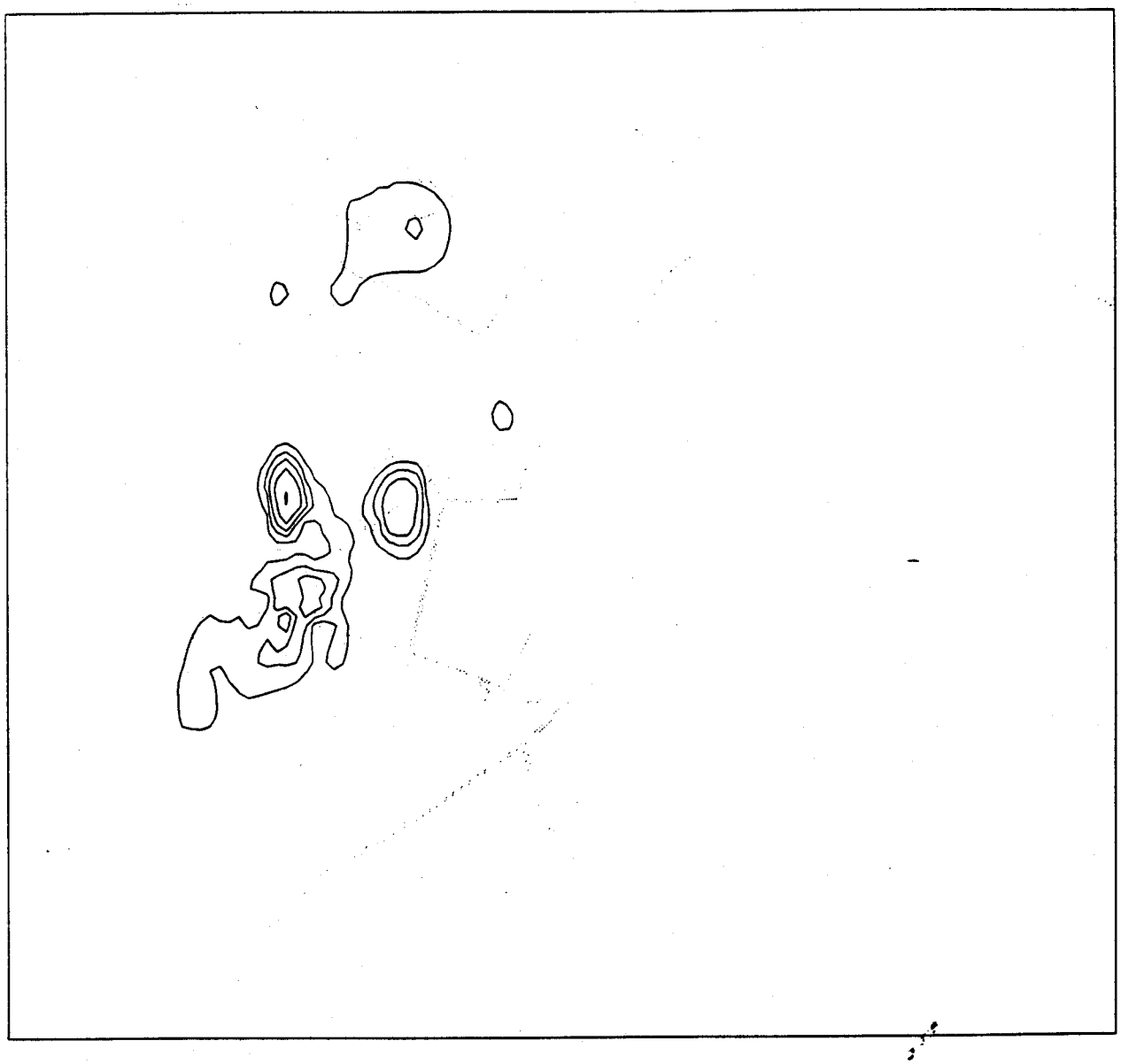

— 20 — Concentration in ppb.

• Well.

2000 0 2000 4000 ft

Figure 10 Concentration in the lower node of layer 2 (2003). Contours are in 20, 50, 100, 200, 500, 1000, and 2000 ppb (Run B1).

14

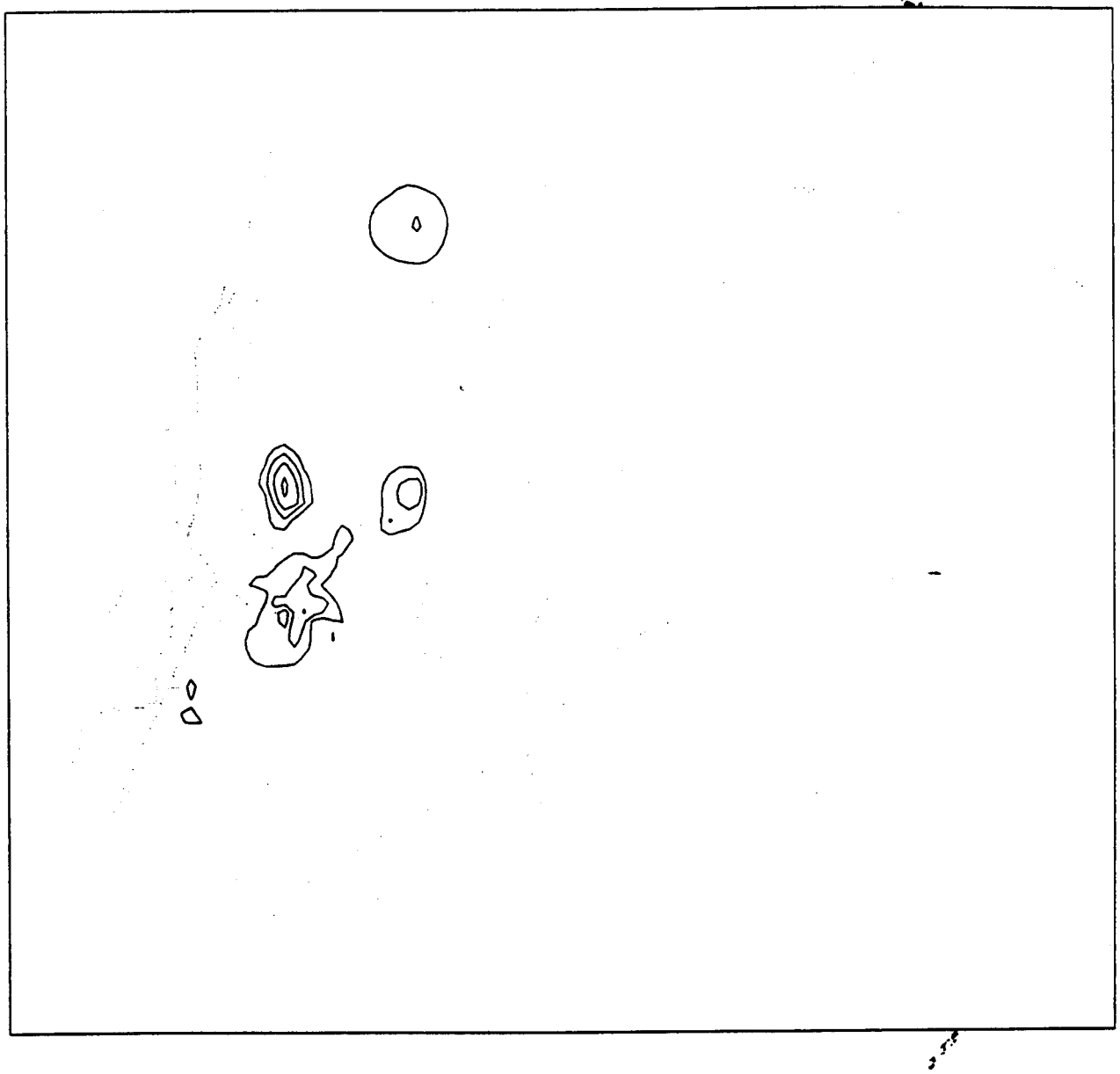

— 20 — Concentration in ppb.

• Well.

2000 0 2000 4000 ft

Figure 11 **Concentration in the upper node of layer 3 (2003). Contours are in 20, 50, 100, 200, 500, 1000, and 2000 ppb (Run B1).**

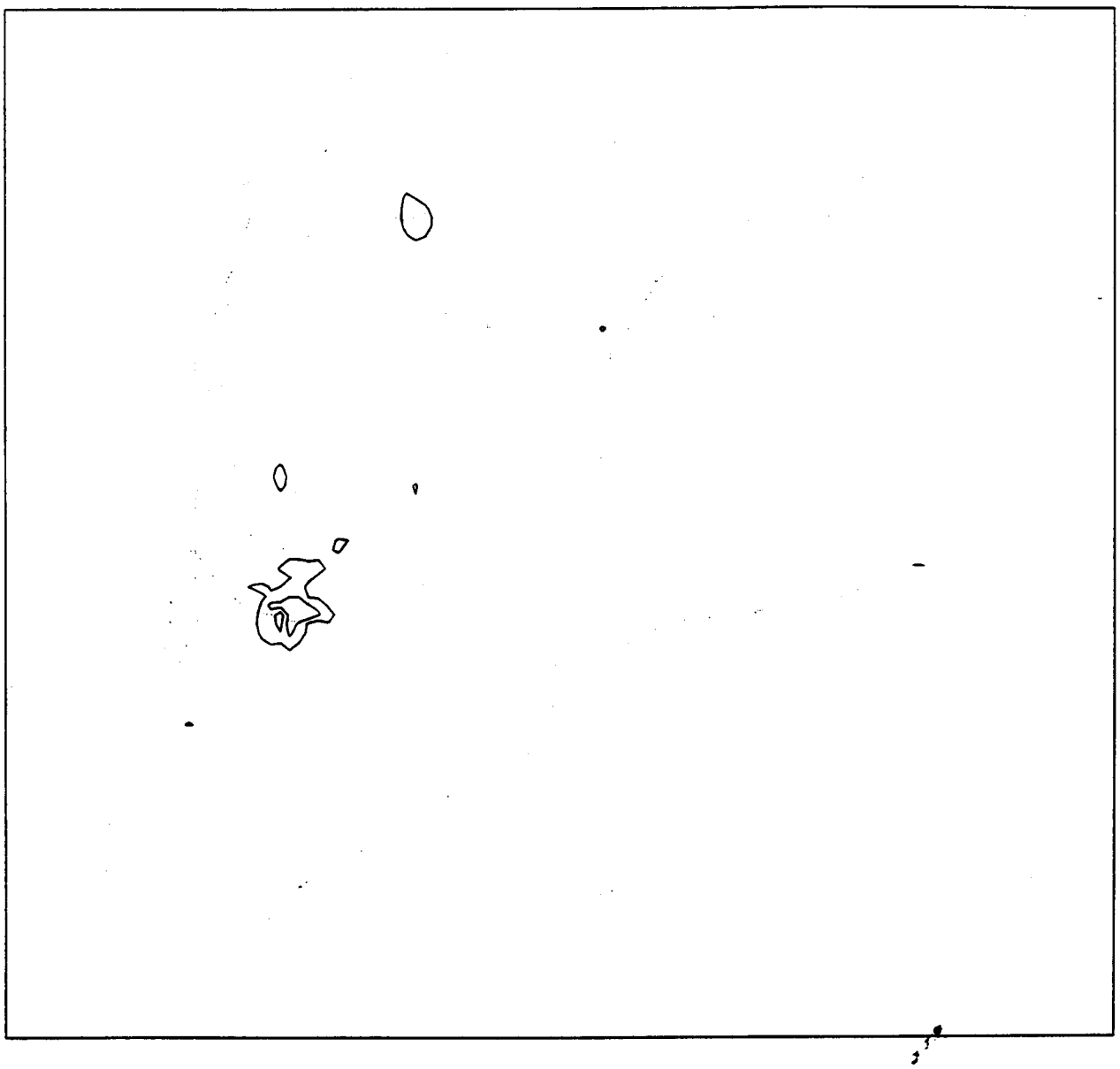

— 20 — Concentration in ppb.

• Well.

2000 0 2000 4000 ft

Figure 12 Concentration in the Lower node of layer 3 (2003). Contours are in 20, 50, 100, 200, 500, 1000, and 2000 ppb (Run B1).

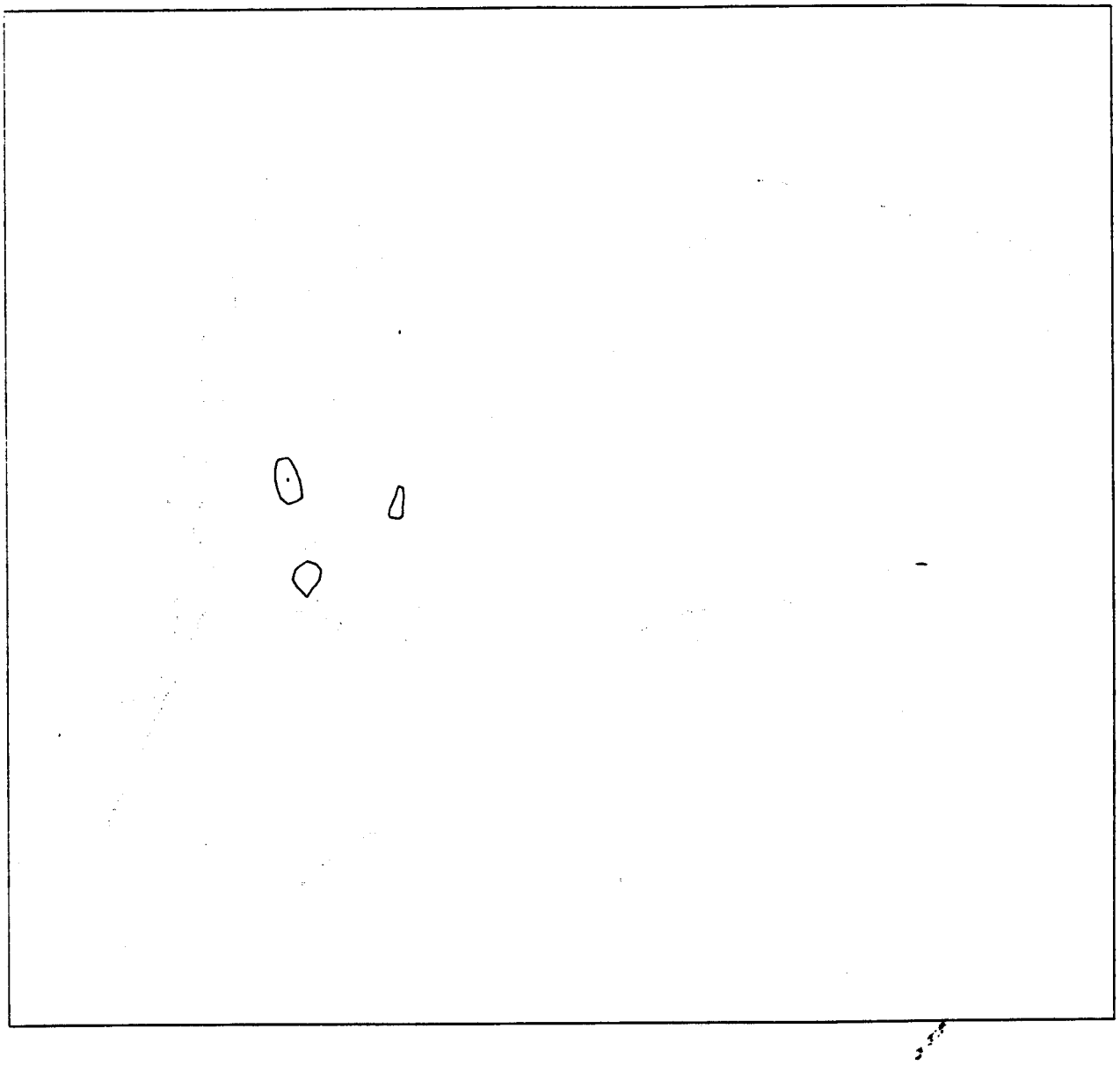

— 20 — Concentration in ppb.

• Well.

2000 0 2000 4000 ft

Figure 13 Concentration in the upper node of layer 2 (2006). Contours are in 20, 50, 100, 200, 500, 1000, and 2000 ppb (Run B1).